Pergamon

Cement and Concrete Research 29 (1999) 1347–1358

CEMENT AND CONCRETE RESEARCH

# Crystallization in pores

George W. Scherer*

*Princeton University, CEE/PMI, Eng. Quad. E-319, Princeton, NJ 08544, USA*

Received 10 August 1998; accepted 28 December 1998

## Abstract

This review discusses the thermodynamics of crystallization within porous materials and the factors that influence stress development and cracking. The maximum driving force for crystallization is related to the supersaturation for crystals growing in solution, and to the undercooling for crystals growing from a melt. However, the stresses generated on the pore walls depend on other factors, including the pore size, the energy ($\gamma_{cs}$) of the interface between the pore wall and the crystal, and (for acicular crystals) the yield stress or buckling strength of the crystal. The fact that growing crystals push particles over large distances indicates that $\gamma_{cs}$ is often large. If $\gamma_{cs}$ were small, crystals would tend to nucleate on pore walls rather than pushing them away, and the crystals would propagate through the pore network without resistance. Even when the crystallization pressure is large, the stress existing in a single pore cannot cause failure because it acts on too small a volume. For fracture to occur, the crystals must propagate through a region of the network large enough that the stress field can interact with the large flaws that control the strength. In concrete, growth on this scale requires that the driving force be sufficient to permit the crystals to pass through pores as small as the breakthrough radius (which is the size of the entry into the percolating network of larger pores that controls the permeability of the body).

*Keywords:* Thermodynamic calculations; Degradation; DEF, Salt crystallization

## 1. Introduction

Growth of salt crystals in the pores of stone or masonry generates stresses that can lead to serious damage [1,2]; similarly, growth of ice is a major cause of deterioration [3]. In many cases, it is not feasible to prevent the ingress of the crystallizing solution, so it is essential to prevent the nucleation and growth of crystals or to provide protection that allows the porous material to accommodate crystallization without harm. To do this, it is necessary to understand the mechanisms by which damage is produced. For example, recognition of the role of hydraulic pressure in freeze/thaw damage [4] led to the introduction of air voids into concrete. To protect natural materials or existing structures that are experiencing deterioration, the only recourse (if ingress cannot be stopped) has been to apply a coating that provides strength or water-repellent properties [5]; we will argue that it would be useful to provide a coating that reduces the interfacial energy between the crystal and the pore wall.

In this review, we examine the mechanisms by which stress is generated in a porous body, with particular attention on the processes occurring at the interface between the crystal and the pore wall. The interfacial energy is shown to play a central role in such seemingly diverse phenomena as crystallization pressure, particle pushing by crystals, and heterogeneous nucleation. Whereas the upper bound on the crystallization pressure is set by the supersaturation (for salt) or undercooling (for ice), there are lower bounds related to the interfacial energies and pore sizes in the system; for acicular (needlelike) crystals, the yield stress or buckling stress must be considered. The pressure in a single pore does not indicate whether cracks will grow; the crystals must exert stress within a volume large enough to contain a strength-limiting flaw, so gross damage is not expected until the crystals propagate through the pore space.

## 2. Theoretical background

The thermodynamics of crystal growth has been thoroughly analyzed over the last century [6–8], so the general principles are well understood. However, there are many issues that have not been clearly discussed in the literature, including how stress is exerted at the interface between a crystal and a pore wall, how the interfacial energies and pore size distribution influence the stress, and how the stress relates to crack growth. These and other issues are addressed in this section. The implications for control of damage from crystallization (of ice, ettringite, etc.) are discussed later.

---

* Corresponding author. Tel.: 1 609 258 5680; fax: 1 609 258 1563.
*E-mail address*: scherer@princeton.edu (G.W. Scherer)

0008-8846/99/$ – see front matter
PII: S0008-8846(99)00002-2

### *2.1. Driving force for crystallization from the melt*

#### *2.1.1. Hydrostatic pressure*

A large crystal of ice immersed in water at 0°C has no tendency to grow or melt, because the chemical potentials of the ice and water are equal. If the temperature is decreased, then the ice tends to grow, because its chemical potential is lower than that of the water. To prevent it from growing, it is necessary to impose a compressive stress on the crystal. The chemical potentials of the liquid and crystal ($\mu_l$ and $\mu_c$) are related to their respective molar volumes ($v_l$ and $v_c$) and molar entropies ($S_l$ and $S_c$) by the Gibbs-Duhem equation [9]:

$$d\mu_l = -S_l dT + v_l dp_l \tag{1a}$$

$$d\mu_c = -S_c dT + v_c dp_c \tag{1b}$$

At equilibrium, $d\mu_l = d\mu_c$; if pressure is applied to the crystal but not to the liquid ($dp_l = 0$), then Eq. (1) requires Eq. (2):

$$\int_{p_e}^{p_A} dp_c = \int_{T_m}^{T} \left(\frac{S_c - S_l}{v_c}\right) dT \tag{2}$$

where $T_m$ is the melting point of a large, unstressed crystal at pressure $p_e$ (the pressure of the triple point, where liquid, crystal, and vapor are in equilibrium) and $T$ is the equilibrium melting temperature under applied pressure $p_A$; thus :

$$p_A - p_e = \int_{T}^{T_m} \Delta S_{fv} dT \approx \Delta S_{fv} \Delta T \tag{3}$$

where $\Delta S_{fv} = (S_l - S_c)/v_c$ is the entropy of fusion per unit volume of crystal (>0); the approximation applies when the undercooling, $\Delta T = T_m - T$ is not too large. This equation means that the work done by the mechanical pressure is equal to the free energy difference between the crystal and liquid, so the growth is arrested. Since $\Delta S_{fv} = 1.2$ J/cm$^3$ • K for ice [10], it requires a pressure of 1.2 MPa per degree of undercooling to prevent the crystal from growing.

#### *2.1.2. Curvature*

A small crystal experiences compressive stress as a result of its surface energy. If the curvature of the crystal/liquid interface ($\kappa_{cl}$) is given by Eq. 4:

$$\kappa_{cl} = \frac{1}{r_1} + \frac{1}{r_2} \tag{4}$$

where $r_1$ and $r_2$ are the principal radii of curvature, then the capillary pressure inside the crystal ($p_c$) is given by Laplace's equation [9,11,12]:

$$p_c = p_l + \gamma_{cl}\kappa_{cl} \tag{5}$$

where $p_l$ is the pressure in the liquid. [The radius of curvature is defined as positive when the center of curvature lies within the body, as it does in a spherical crystal; for a concave crystal, the center of curvature is outside the body, and the curvature is negative.] The energy of the water/ice interface is estimated to be ~0.04 J/m$^2$ [13], so a pressure of 1.2 MPa would exist in a spherical crystal with a radius of $r_1 = r_2 \approx 67$ nm. From Eqs. (3) and (5) we find that (when $p_l = p_e$) the equilibrium melting point for such a crystal differs from that of a large flat crystal

$$\Delta T \approx \frac{\gamma_{cl}\kappa_{cl}}{\Delta S_{fv}} \tag{6}$$

This indicates that the equilibrium melting temperature of a crystal with a positive curvature is lower than that of a large flat crystal; a spherical crystal of ice with a radius of 67 nm would melt at any temperature above −1°C.

#### *2.1.3. Polyhedral crystals*

Many crystals have anisotropic surface energies, with a unique value $\gamma_i$ for the *i*th family of crystal planes. In such cases, the equilibrium shape for the crystal is not a sphere, but a polyhedron called the Wulff shape: if the distance from the centroid of the crystal to the face of type $i$ is $r_i$, then at equilibrium the quantity $\gamma_i/r_i$ is a constant [12]. Therefore, for a polyhedral crystal, Eq. (5) becomes Eq. (7):

$$p_c = p_l + \frac{2\gamma_i}{r_i} \tag{7}$$

where $i$ can refer to any of the faces of the crystal, and $r_i$ is the radius of the inscribed circle tangent to the face with surface energy $\gamma_i$. As a simple illustration, consider a cubic crystal (such as NaCl). To find the work that would have to be done to cause a change in surface area of the crystal, we would write

$$p_c dV = \sum_{i=1}^{N} \gamma_i dA_i = 6\gamma_1 dA_1 \tag{8}$$

where the sum is over all types of faces in the crystal, and the second equality reflects the fact that all six faces of the cube are identical. If the distance from the centroid of the crystal to the face is $r_1$, then $A_1 = 4\,r_1^2$ and $dA_1 = 8r_1dr_1$; the volume of the crystal is $V = 8r_1^3$, so $dV = 24r_1^2\,dr_1$, and Eq. (8) leads to Eq. (9):

$$p_c = \frac{6\gamma_1(8r_1dr_1)}{24r_1^2dr_1} = \frac{2\gamma_1}{r_1} \tag{9}$$

An equivalent result would be obtained for a parallelepiped with faces at distances $r_1$, $r_2$, and $r_3$ from the centroid; in that case, the pressure can be written as $2\gamma_i/r_i$ with $i = 1$, 2, or 3, since the ratio is identical for all faces in a crystal with the equilibrium (Wulff) shape. In the remainder of this paper we will relate the thermodynamics of the crystal to its curvature, without further reference to the actual crystal shape, recognizing that equivalent expressions can be written in terms of the quantity $\gamma_i/r_i$ for polyhedral crystals.

#### *2.1.4. Nonhydrostatic stress*

Suppose that a cubic crystal is subjected to mechanical stresses $\sigma_x$ and $\sigma_y$ on the faces perpendicular to the $x$ and $y$ axes, respectively, and is exposed to a melt on the $z$ face; there is no mechanical load on the $z$ face, but it is in contact with a liquid at pressure $p_l$. Gibbs [7] showed (see Appendix) that the melting point is shifted according to Eq. (10):

$$\Delta S_{fv} dT = -\sigma_x d\epsilon_x - \sigma_y d\epsilon_y \tag{10}$$

where $\epsilon_x$ and $\epsilon_y$ are the elastic strains along the $x$ and $y$ axes. (The negative sign in front of $\sigma_r$ is required by the convention that compressive pressure is positive, but compressive stress is negative.) If $\sigma_x = \sigma_y$, and the crystal obeys Hooke's law, then [see Eq. (11)]

$$\int_{T_m}^{T} \Delta S_{fv} dT = -\int_0^{\sigma_x} 2\sigma_x d\epsilon_x = -\int_0^{\sigma_x} 2\sigma_x\left(\frac{1-\nu}{E}\right) d\sigma_x \tag{11}$$

where $E$ is Young's modulus and $\nu$ is Poisson's ratio. The result for a crystal under biaxial stress is

$$\frac{(1-\nu)\sigma_x^2}{E} = \int_T^{T_m} \Delta S_{fv} dT \approx \Delta S_{fv} \Delta T \tag{12}$$

For ice, $E \approx 9$ GPa and $\nu \approx 0.33$ [14], and $\Delta S_{fv} = 1.2$ MPa/°C, so a stress of $\sigma_x \approx 127$ MPa would be required to reduce the melting point by 1°C. This is very different from the effect of pressure described by Eq. (3), because Eq. (12) refers to the change in melting point of the unstressed face that is in contact with the melt; the stressed face is *not* in contact with the melt.

Gibbs showed [7, p. 196] that if different faces of a given crystal are subjected to different pressures, then equilibrium requires that the chemical potentials (free energy per mole) of the liquids in contact with those faces must differ

$$\Delta\mu = v_c \Delta p_c \tag{13}$$

In the example of the preceding paragraph, the difference in pressure applied to the $x$ and $z$ faces is $\Delta p_c = \sigma_x$, so if both faces were exposed to the melt, then the temperatures of the liquids in equilibrium with each face would differ by

$$\Delta T = \frac{\sigma_x}{\Delta S_{fv}} \tag{14}$$

Thus, for ice, the temperature of the liquid would have to differ by 1°C for every 1.2 MPa difference in applied stress ($\Delta T < 0$ for compressive stress, $\sigma_x < 0$). Consequently, if both the stressed and unstressed faces were exposed to the same liquid, then there would be no equilibrium. For example, if the temperature is held at $T_m$ (so that an unstressed crystal is in equilibrium), then a compressed face will melt according to Eq. (14); moreover, the unstressed face will melt according to Eq. (12). In an adiabatic system, the melting of the stressed face will tend to lower the temperature of the liquid, leading to growth of crystal on the unstressed face (which has a smaller $\Delta T$ than the stressed face). If the unstressed face acquired a curvature (as illustrated in Fig. 1) such that [see Eq. (15)]

$$p_c = p_l + \gamma_{cl}\kappa_{cl} = -\sigma_x \tag{15}$$

then the crystal would be in *mechanical* equilibrium, because the pressure from the curvature would be equal to the applied mechanical load, so the crystal would be under a uniform hydrostatic pressure. However, both faces are at temperature $T_m$, so the crystal would melt away while retaining a uniform curvature; if $T$ were reduced so as to satisfy Eq. (6), then the crystal would be in equilibrium, and the shape in Fig. 1 would be stable.

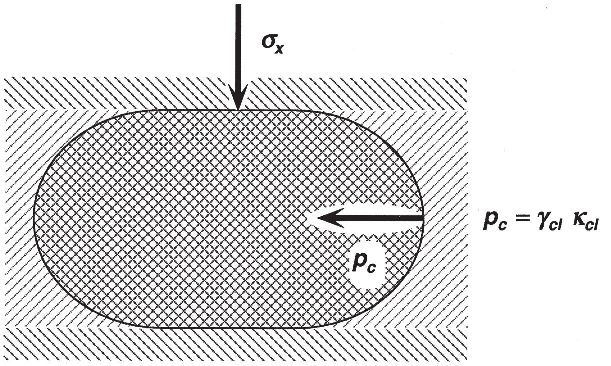

Fig. 1. Crystal subjected to a uniaxial mechanical stress $\sigma_x$ is in equilibrium when the curvature of the unloaded faces satisfies Eq. (15).

### 2.2. Driving force for crystallization from solution

For crystals growing from solution, the chemical potential difference between the crystal and the liquid is [12]

$$\Delta\mu = R_g T \ln(a/a_0) \tag{16}$$

where $R_g$ is the ideal gas constant, $a$ is the activity of the solution, and $a_0$ is the activity of a solution in equilibrium with a large crystal. If the activity coefficients are ignored, Eq. (16) can be written in the approximate form

$$\Delta\mu = R_g T \ln(C/C_0) \tag{17}$$

where $C$ is the concentration of solute and $C_0$ is the equilibrium solubility. If the solution is supersaturated ($C > C_0$), then the hydrostatic pressure that would have to be applied on the crystal to suppress its growth is

$$p_c = p_l + \frac{R_g T}{v_c}\ln(C/C_0) \tag{18}$$

For sodium chloride ($v_c = 24.55$ cm$^3$/mole), the pressure would have to be ~30 MPa to suppress growth at 20°C if $C/C_0 = 2$ (i.e., if the solution is supersaturated by a factor of two). Supersaturation of that magnitude can easily result from evaporation of water from a solution, so very large pressures could be required to suppress the growth of a crystal in a pore.

A small crystal is under pressure caused by its surface energy, so Eqs. (5) and (18) indicate that equilibrium requires

$$\gamma_{cl}\kappa_{cl} = \frac{R_g T}{v_c}\ln(C/C_0) \tag{19}$$

This means that a small spherical crystal is in equilibrium with a higher concentration than a large flat crystal. For example, if $\gamma_{cl} = 0.1$ J/m$^2$, then a crystal with radius $\sim$6.7 nm would be in equilibrium with a twofold supersaturation and would be under a capillary pressure of $\sim$30 MPa.

If each face of a crystal were subjected to a different pressures, then each face would be in equilibrium with a solution of a different concentration. According to Eqs. (13) and (17), the pressures and concentrations would be related by

$$\Delta p_c = \left(\frac{R_g T}{v_c}\right)\Delta \ln\left(\frac{C(p_c)}{C_0}\right) \tag{20}$$

If the pressure is $\sigma_x$ on one face and $\sigma_y$ on another, then Eq. (20) becomes Eq. (21):

$$\sigma_x - \sigma_y = \left(\frac{R_g T}{v_c}\right)\ln\left[\frac{C(\sigma_x)}{C(\sigma_y)}\right] \tag{21}$$

or Eq. (22):

$$C(\sigma_x) = C(\sigma_y)\exp\left[-\frac{(\sigma_x - \sigma_y)v_c}{R_g T}\right] \tag{22}$$

Now, if $\sigma_y = p_l$, then $C(\sigma_y) = C_0$ and Eq. (22) reduces to Eq. (23):

$$C(\sigma_x) = C_0\exp\left[-\frac{\sigma_x v_c}{R_g T}\right] \tag{23}$$

For sodium chloride, if $\sigma_x = -30$ MPa then $C(\sigma_x) \approx 2C_0$; if a crystal in a solution with concentration $C_0$ were under a compressive uniaxial load of this magnitude, the loaded face would dissolve, and the solute would precipitate onto the unloaded face. Mechanical equilibrium would be restored, as in Fig. 1, if the unloaded face acquired a curvature $\kappa_{cl}$ such that $\sigma_x = -\gamma_{cl}\,\kappa_{cl}$; if the concentration of the liquid remained below $2C_0$, then the crystal would dissolve, but if dissolution raised the concentration of the liquid to $2C_0$, then equilibrium would prevail and dissolution would stop.

### 2.3. Growth into a pore

Fig. 2 shows the shape of a crystal entering a cylindrical pore whose radius is $r_p$. The contact angle between the crystal and the pore wall is $\theta$, and the curvature of the crystal/liquid interface is [9]

$$\kappa_{cl} = -\frac{2\cos(\theta)}{r_p} \tag{24}$$

According to Eq. (5), the capillary pressure in the crystal is

$$p_c - p_l = -\frac{2\gamma_{cl}\cos(\theta)}{r_p} \tag{25}$$

If $\theta > 90°$, then $\cos(\theta) < 0$, so the pressure is positive and the equilibrium melting point is reduced according to Eq. (6). The maximum pressure in the crystal occurs in cases where $\theta = 180°$ (i.e., where the crystal is completely *nonwetting*, making no contact with the wall); in such cases, Eq. (25) should be modified to take account of the thickness ($\delta$) of the unfrozen film as shown in Eq. (26)

$$p_c - p_l = \frac{2\gamma_{cl}}{r_p - \delta} \tag{26}$$

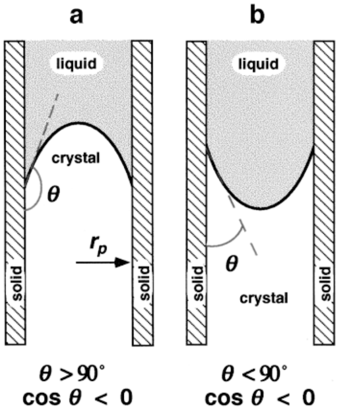

Fig. 2. Shape of crystal entering a cylindrical pore with radius $r_p$; the contact angle between the crystal and the pore wall is $\theta$. (a) $\theta > 90°$; (b) $\theta < 90°$.

If $\theta > 90°$, a crystal cannot enter a pore at $T_m$, and the smaller the pore, the lower the temperature that is required to permit entry; from Eqs. (6) and (24), the crystal can enter the pore when [see Eq. (27)]

$$\Delta T \approx -\frac{2\gamma_{cl}\cos(\theta)}{r_p \Delta S_{fv}} \tag{27}$$

On the other hand, if the contact angle is $<90°$, then $\cos(\theta) > 1$, and the melting point is not depressed. In such cases, the crystal can freely enter the pore at the usual melting point; in fact, Eq. (27) indicates that the crystal would be stable against melting above $T_m$ [15]. In general we expect $\theta > 90°$, so that crystals do not propagate through a porous material unless undercooled; however, if there were a porous material such that $\theta \leqslant 90°$, then crystals would propagate through the pores at $T_m$ without resistance.

### 2.4. Particle pushing

It has long been known that crystals can push away particles suspended in the liquid [16]. Corte [17] showed that ice could lift a heavy load of particles, indicating that a liquid film was sustained between the crystal and the particles as the ice advanced; he also found that there was a critical growth velocity beyond which a particle would be captured by the ice, and the critical velocity was greater for smaller particles. These phenomena were explained by Uhlmann et al. [18], who pointed out that there can be a repulsive interaction between the crystal and particle arising from interfacial energy: if the energy of the interface between the particle and the crystal ($\gamma_{cs}$) is greater than the sum of the energies of the crystal/liquid ($\gamma_{cl}$) and particle/liquid ($\gamma_{sl}$) interfaces, then the energy of the system would increase if contact occurred. That is, there is a chemical potential proportional to $\gamma_{cs} - (\gamma_{cl} + \gamma_{sl})$ available to prevent contact. This chemical potential draws liquid into the gap between the crystal and the particle, allowing the crystal to continue growing and pushing the particle away. However, if the growth rate is too high, then the available chemical potential

Table 1
van der Waals interaction energies between ice and various oxides

| Substance | ε[a] | $n$[b] | $A_{123}$[c] ($10^{-21}$ J) | $p$[d] (MPa) |
|---|---|---|---|---|
| Water[e] | 80 | 1.333 | – | – |
| Ice[f] | 110 | 1.309 | +1.00 | +11.8 |
| Quartz[e] | 3.8 | 1.448 | −1.20 | −14.2 |
| Mica[e] | 7.0 | 1.60 | −2.11 | −24.9 |
| Alumina[e] | 11.6 | 1.75 | −2.94 | −34.7 |

[a]Static dielectric constant; [b]refractive index; [c]Hamaker constant for interaction of ice with substance in first column through water, from Eq. (28); [d]pressure calculated from Eq. (32); negative values indicate repulsion; [e]data from [19]; [f]Data from R.C. Weast and M.J. Astle, eds., CRC Handbook of Chemistry and Physics, 62d ed., CRC Press, Boca Raton, FL, 1981.

is not sufficient to suck liquid into the gap fast enough; in that case, the crystal cannot grow as fast behind the crystal as it can where no particles are present, so the crystal engulfs the particle (i.e., the critical velocity is exceeded). The larger the particle, the more difficult it is to provide a sufficient flow of liquid into the gap, so the critical velocity is lower for larger particles. This phenomenon is the cause of frost heave [15,17], where large crystals of ice grow in pockets of water and push soil particles out of the way; the pressures that can be generated are great enough to damage roadways and they result entirely from the interfacial incompatibility of ice and soil.

The fact that crystals can push particles over long distances clearly indicates that there is a film of liquid between them. The repulsive forces acting within the film can be of several kinds. A repulsion can result entirely from van der Waals forces when two different solids are separated by a liquid, but this requires that the Hamaker constant of the liquid lie between those of the two solids [19]. The latter situation is commonly observed in organic systems [20], and the tendency of a crystal to push or engulf a particle correlates extremely well with the difference in interfacial energies in such systems [21]. The force of interaction of condensed phases 1 and 3 across a liquid medium 2 depends on the Hamaker constant, $A_{123}$; a useful approximation is provided by the following formula [19, p. 184]:

$$A_{123} \approx \frac{3kT}{4}\left(\frac{\epsilon_1-\epsilon_3}{\epsilon_1+\epsilon_3}\right)\left(\frac{\epsilon_2-\epsilon_3}{\epsilon_2+\epsilon_3}\right) + \frac{3h\nu_e}{8\sqrt{2}}\frac{(n_1^2-n_3^2)(n_2^2-n_3^2)}{(n_1^2+n_3^2)(n_2^2+n_3^2)[(n_1^2+n_3^2)^{1/2}+(n_2^2+n_3^2)^{1/2}]} \tag{28}$$

where $k$ = Boltzmann's constant, $h$ = Planck's constant, $\nu_e$ = main electronic absorption frequency in the ultraviolet ($\approx 3 \times 10^{15}$ s$^{-1}$), and $\epsilon_j$ and $n_j$ are the static dielectric constant and refractive index of phase $j$. Taking ice as phase 1 and water as phase 2, we can find $A_{123}$ for a variety of solids, with the results shown in Table 1; the negative values indicate that an ice crystal would repel the oxides listed there, although it would attract a particle of ice. The energy of interaction $W$ between a particle of radius $R$ and a planar ice crystal at a separation of $D$ is given by [19, p. 177]:

$$W = -\frac{AR}{6D} \tag{29}$$

The resulting pressure exerted on the particle is approximately

$$p_{vdw} \approx \frac{1}{\pi R^2}\frac{dW}{dD} \approx \frac{A_{123}}{6\pi R D^2} \tag{30}$$

The pressure exerted by a particle owing to gravity is approximately

$$p_{grav} \approx \frac{\rho g(4\pi R^3/3)}{\pi R^2} \approx \frac{4\rho g R}{3} \tag{31}$$

For a 10-μm particle of quartz, the gravitational pressure given by Eq. (31) is less than that given by Eq. (30) for any separation $D < 4$ nm, so the ice could easily lift such a particle just by van der Waals repulsion; the ice would ride on a film of water a few nanometers thick.

The Hamaker constant given by Eq. (28) also is related to the pressure that would be required to push planar surfaces of materials 1 and 3 into contact, displacing liquid material 2, [19, p. 197]:

$$p = \frac{A_{123}}{6\pi D_0^3} \tag{32}$$

where $D_0$ is the distance of closest approach ($D_0 \approx 0.165$ nm). Table 1 shows that the pressure required to push ice into contact with several oxides is on the order of tens of MPa, and this calculation takes account only of the van der Waals forces.

The values of surface tension calculated from the Hamaker constant are accurate for nonpolar liquids, such as alkanes, but are underestimates for polar liquids, metals, and other materials for which the van der Waals forces make a minor contribution to bonding [19]. For such materials, hydrogen bonding and other factors dominate the surface energy, so that the energies calculated from Eq. (29) may represent a small part of the repulsion (or attraction) between materials; for water, van der Waals interactions are responsible for only ~25% of the surface energy [19]. All of these factors (such as polar interactions) are capable of exerting force across a film of liquid, so they permit a crystal to detect and repel (or attract) an obstacle, such as a particle. Similarly, these forces allow a crystal to detect the presence of a pore wall before making physical contact; if the interaction is repulsive, the crystal tries to push the wall away, just as it would push a particle of the same substance. Just as the crystal would sustain a film of liquid between itself and the particle, it will sustain a film between itself and the pore wall.

The ability of a crystal to repel a particle is enhanced by disjoining forces, such as the hydration forces created by ordered layers of water molecules [19] and by electrostatic repulsion [22]. The width of the gap between the crystal and particle is likely to be small enough that electrostatic forces are less important than hydration forces, which predominate within a few nanometers of a surface; this is particularly true at the high salt concentrations required for precipitation of crystals from solution.

### 2.5. Stress on the pore wall

Fig. 2 shows crystals advancing into cylindrical pores with different contact angle, θ. The energy of the crystal is minimized if the curvature of the advancing surface of the crystal is [9]

$$\kappa_{cl} = -\frac{2\cos(\theta)}{r_p} \tag{33}$$

If $\theta = 180°$, then the tip of the crystal is hemispherical and there may be a film of liquid between the crystal and the wall; for any $\theta < 180°$, there is direct contact of the crystal with the wall. According to Eq. (5), the capillary pressure inside the crystal is [Eq. (34)]

$$p_c = p_l - \frac{2\gamma_{cl}\cos(\theta)}{r_p} \tag{34}$$

When $\theta > 90°$, as in Fig. 2*(a)*, then $\cos(\theta) < 0$ and $p_c > 0$; therefore, according to Eq. (27), the crystal cannot enter the pore unless $T < T_m$. On the other hand, if $\theta < 90°$, as shown in Fig. 2*(b)*, then $\cos(\theta) > 0$ and $p_c < 0$, so the crystal can freely invade the pore when $T = T_m$.

The crystal shown in Fig. 3 has a tip whose curvature is given by Eq. (33), but the sides of the crystal are cylindrical, so their curvature is $1/r_p$; the resulting capillary pressure is $\gamma_{cs}/r_p$. At equilibrium, the pressure inside the crystal must be uniform; otherwise, material would melt or dissolve from the region of higher pressure and deposit elsewhere. To achieve equilibrium in a crystal in a pore, the walls exert the additional pressure required to balance the difference in capillary pressure. The radial stress exerted by the wall on the crystal, $\sigma_r$, is found by equating the pressures at the tip and the sides of the cylindrical crystal:

$$p_l - \frac{2\gamma_{cl}\cos(\theta)}{r_p} = \frac{\gamma_{cs}}{r_p} - \sigma_r \tag{35}$$

Thus, the radial stress on the pore wall is

$$\sigma_r = \frac{\gamma_{cs} + 2\gamma_{cl}\cos(\theta)}{r_p} - p_l \tag{36}$$

The interfacial energies are related by Young's equation or Eq (37) [12],

$$\gamma_{sl} = \gamma_{cs} + \gamma_{cl}\cos(\theta) \tag{37}$$

so Eq. (36) can be written as

$$\sigma_r = \frac{\gamma_{cl}\cos(\theta)}{r_p} + \frac{\gamma_{sl}}{r_p} - p_l \tag{38}$$

Now, there is a tensile radial stress on the pore wall *before* the crystal enters, because of the pressure in the pore liquid and the curvature of the pore surface, and the magnitude of that stress is given by the last two terms in Eq. (38). Therefore, the *change* in stress on the wall as the crystal enters the pore is

$$\Delta\sigma_r = \frac{\gamma_{cl}\cos(\theta)}{r_p} \tag{39}$$

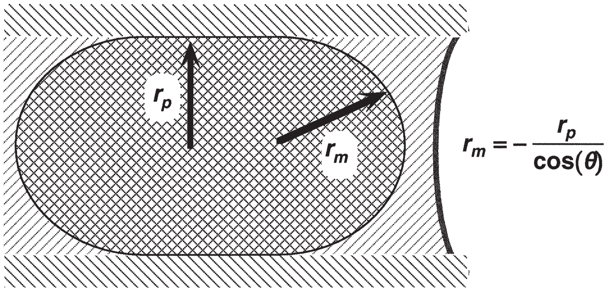

Fig. 3. Crystal in cylindrical pore has nonuniform curvature, since the radius of the tip is $r_m = -r_p/\cos(\theta)$ and the sides are cylindrical with radius $r_p$.

When $\theta = 90°$, then the tip of the crystal is flat, so its internal pressure is just $p_l$; in that case, Eq. (36) indicates that the stress on the pore wall is $\sigma_r = \gamma_{cs}/r_p - p_l$. This means, as indicated by Eq. (39), that $\sigma_r$ does not change when the crystal enters the pore (i.e., $\gamma_{cs} = \gamma_{sl}$ and $\Delta\sigma_r = 0$). However, if $\theta > 90°$, then the wall feels an additional radial compression caused by the crystal.

The greatest compression occurs when $\theta = 180°$, when a film of liquid is present at the interface between the crystal and pore wall. In that case, taking account of the thickness of the unfrozen layer, the pressure at the tip of the crystal is $p_l + 2\gamma_{cl}/(r_p - \delta)$ and the pressure on the cylindrical sides is $\gamma_{cl}/(r_p - \delta) + p_l$, so Eq. (35) is replaced by Eq. (40)

$$p_l + \frac{2\gamma_{cl}}{r_p - \delta} = \frac{\gamma_{cl}}{r_p - \delta} + p_l - \sigma_A,\ \theta = 180° \tag{40}$$

which indicates that [see Eq. (41)]

$$\sigma_A = -\frac{\gamma_{cl}}{r_p - \delta}, \theta = 180° \tag{41}$$

where $\sigma_A$ is the stress exerted on the side of the crystal by the wall. The total radial stress on the wall includes contributions from $\sigma_A$, the pressure in the liquid, and the capillary pressure from the solid-liquid interface:

$$\sigma_r = \frac{\gamma_{sl}}{r_p} - p_l + \sigma_A = \frac{\gamma_{sl}}{r_p} - \frac{\gamma_{cl}}{r_p - \delta} - p_l, \theta = 180° \tag{42}$$

where the second equality follows from Eq. (41). The change in stress on the wall when the crystal enters the pore is analogous to Eq. (39): $\Delta\sigma_r = -\gamma_{cl}/(r_p - \delta)$.

The compressive radial stress is accompanied by a tensile hoop stress, $\sigma_\theta$, in the pore wall, and it is the tensile stress that can cause damage to the body. If we model the pore as a cylindrical tube with inner radius $r_p$ and outer radius $b$, then the hoop stress at the surface of the pore is [23]:

$$\sigma_\theta = -\sigma_r\left(\frac{b^2 + r_p^2}{b^2 - r_p^2}\right) \tag{43}$$

The porosity, $P$, of such a structure would be $P = (r_p/b)^2$, so Eq. (43) could be written as

$$\sigma_\theta = -\sigma_r\left(\frac{1+P}{1-P}\right) = \left(p_l - \frac{\gamma_{sl} + \gamma_{cl}\cos(\theta)}{r_p}\right)\left(\frac{1+P}{1-P}\right) \tag{44}$$

where the second equality follows from Eq. (38). Of course, Eq. (43) is based on a crude microstructural model; if the pores were represented as spheres, rather than cylinders, the relationship between $\sigma_r$ and $\sigma_\theta$ would be different [9]. In the limit of low porosity, Eq. (43) indicates that $\sigma_\theta = -\sigma_r$; the tensile stress increases with $P$. If $\theta = 180°$ and $P$ is small, then Eqs. (42) and (43) indicate that [see Eq. (45)]:

$$\Delta\sigma_\theta\Big|_{P=0}^{\theta=180°} \approx \frac{\gamma_{cl}}{r_p - \delta} \tag{45}$$

Thus, when a liquid film exists between the crystal and the pore wall, the hoop tension in the wall is about half the capillary pressure inside the crystal.

Eq. (44) indicates that the tensile stress in the pore wall is reduced if there is a negative pressure in the liquid. The pressure in the liquid is related to the curvature of the liquid/vapor interface, $\kappa_{lv}$, which is related to the relative pressure of the vapor, $p_v$:

$$p_l = \gamma_{lv}\kappa_{lv} = \frac{R_g T}{v_1}\ln\left(\frac{p_v}{p_{v0}}\right) \tag{46}$$

where $\gamma_{lv}$ is the liquid/vapor interfacial energy. Whenever the relative humidity is below 100% ($p_v/p_{v0} < 1$), then there is a negative pressure in the liquid; this is the case in any unsaturated porous material. The suction in the liquid pulls the body into compression, and the crystal has to overcome that compression in order to do damage.

### 2.6. Acicular crystals

When an acicular (needle-shaped) crystal grows across a pore, it can exert stress at each end of the crystal, as long as there is a driving force for growth and $\gamma_{cs} > \gamma_{cl} + \gamma_{sl}$. Consider the crystal in Fig. 4, with radius $r_1$ and length equal to the pore diameter, $2r_p$; it is growing in a pore filled with a supersaturated solution. The crystal pushes on the wall if the Wulff criterion discussed previously dictates an equilibrium half-length $L > r_p$. The equilibrium radius of a crystal with length $2r_p$ would be $r_1' = r_p\,\gamma_1/\gamma_2$, where $\gamma_1$ is the energy of the lateral crystal/liquid interface and $\gamma_2$ is the energy of the end face. The pressure exerted by the wall to prevent the crystal from increasing its length from $r_p$ to $L$ must be the same as the pressure that would be required to reduce the radius from $r_1$ to $r_1'$, because these changes represent equal departures from equilibrium. Since the internal pressure on every surface of a polyhedral crystal is given by Eq. (7), the pressure exerted by the end of the crystal on the pore wall is

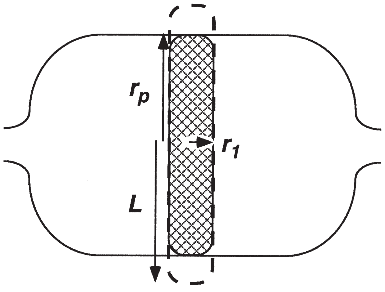

Fig. 4. Acicular crystal with length $2r_p$ and radius $r_1$ growing in pore; the equilibrium half-length is given by the Wulff criterion, $\gamma_1/r_1 = \gamma_2/L$.

$$\sigma_r = 2\gamma_1\left(\frac{1}{r_1} - \frac{1}{r_1'}\right) = \frac{2\gamma_1}{r_1} - \frac{2\gamma_2}{r_p} \tag{47}$$

This stress would be zero if $r_p$ were equal to the equilibrium half-length of the crystal, but it is compressive when $r_p < L$. The stress from Eq. (47) cannot be inserted into Eq. (43), because it is not uniformly applied to the pore wall, but exists only on the surfaces of contact (each with area $\pi r_1^2$).

There are two additional factors that might limit the stress applied on the walls by an acicular crystal: the yield strength ($\sigma_y$) of the crystal and the tendency to buckle. If the crystal yields, then it will spread laterally in the pore, as indicated in Fig. 5(a). If the crystal spreads to the extent that it fills the pore, then the stress it can exert will depend on the curvature of the pore entry, as indicated in Fig. 5(b); the stress in this case is described by the equations given in the previous subsection.

If the crystal does not yield, then it might buckle. The critical stress ($\sigma_{cr}$) at which a long thin crystal buckles is given by the Euler condition, shown in Eq. (48) [24]:

$$\sigma_{cr} = \frac{\pi^2 E}{(h/r)^2} \tag{48}$$

where $E$ is Young's modulus and $h/r$ is the ratio of length to radius of the crystal. When $h/r = 10$, this reduces to $\sigma_{cr} \approx E/10$, which is much greater than the yield stress of most crystals. For ice and alkali halides, the ratio of the yield stress to Young's modulus is ~0.01 [25], so buckling is more likely than shear only if $h/r$ exceeds about 30. In fact, the crystallization pressure is unlikely to exceed the yield stress, since $\sigma_y$ is about 85 MPa for ice and 200–350 MPa for alkali halides [25], and this exceeds the available driving force except at extreme supersaturations or undercoolings.

Thus, it seems that acicular crystals will be able to exert a stress limited only by the driving force and interfacial energy; buckling will occur only for extremely long needles. Of course, the force exerted on the pore wall is not very great if the crystals only touch in a few points. If the same crystal filled a small void so that it could exert force on the whole surface, it could generate a greater stress in the body.

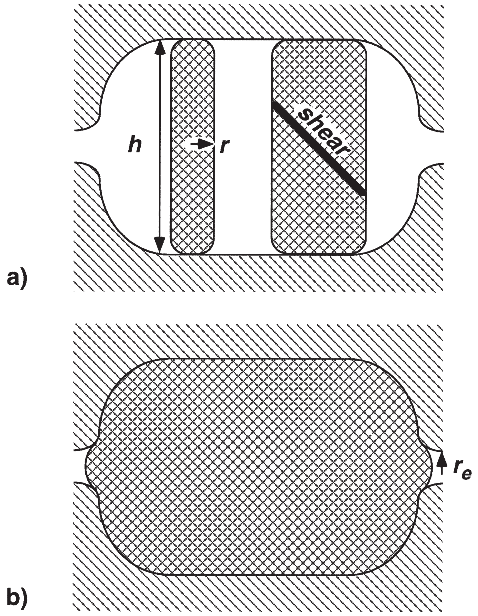

Fig. 5. (a) Acicular crystal with length *h* and radius *r* makes contact with wall; if the crystallization pressure exerted by an acicular crystal exceeds its yield strength, then the crystal will spread laterally, as indicated by the crystal on the right; (b) once it has filled the pore, the pressure will be limited by the radius of the pore entry, $r_e$.

In fact, the formation of long fibrillar crystals may result not from the anisotropy of the crystal, but from the source of solution: If a crystal is nucleated on a porous surface (such as the face of a crack), the capillary suction in the pores may prevent the liquid from flowing over the surface of the crystal, so that it is only available at the point of contact of the crystal with the surface [26]. In such cases, the crystal grows from its base, and can form long whiskers even though relatively equiaxed crystals would form if the crystal were immersed in solution. This phenomenon could be responsible for the growth of long needles of ettringite it cracks.

### *2.7. Nucleation of crystals*

If very pure water is cooled below its melting point, ice does not form spontaneously (i.e., by homogeneous nucleation) until the temperature reaches about −38°C [27]. The reason for this huge departure from equilibrium is that the crystal/liquid interfacial energy ($\gamma_{cl}$) constitutes a barrier to formation of a tiny crystal in a liquid. When ordinary tap water is cooled in our laboratory in a differential scanning calorimeter, it typically freezes at −7 to −15°C; the onset of freezing is also found in this range in studies of freezing in porous materials [28,29]. Therefore, except in the most carefully controlled experiments, freezing of water occurs by heterogeneous nucleation, where a nucleating agent provides a surface with a relatively low interfacial energy ($\gamma_{cs}$) with the crystal (see Fig. 6). When the contact angle is low, concavities (such as cracks and pits) constitute particularly favorable nucleation sites since they maximize contact between the substrate and crystal [30]. For a substrate to be a potent nucleating agent, the contact angle must be less than 90°: as indicated in Fig. 7, the temperature at which nucleation rate of ice becomes appreciable is still about −27°C when $\theta = 90°$; to raise the temperature above −7°C requires $\theta < 35°$.

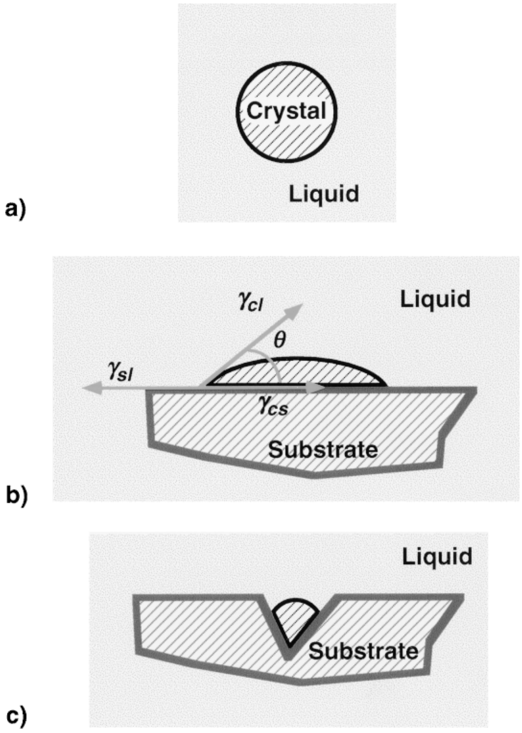

Fig. 6. (a) Homogeneous nucleation requires the formation of a crystal directly from the liquid; (b) heterogeneous nucleation on a substrate is favored when the contact angle, θ, between the crystal and substrate is low; (c) cracks and pits are particularly favorable nucleation sites, as they maximize the contact between substrate and crystal.

If the pore wall itself were an effect nucleating agent ($\theta < 90°$), then the results of the previous section indicate that the crystal would immediately propagate through all of the pores without any further undercooling. When the liquid contained in cement or porous glass is frozen [28,29], or when thermoporometry is employed to measure pore-size distributions [13], only a certain fraction of the pore liquid freezes at a given temperature; further freezing requires a reduction in temperature. This means that advance of the crystals *is* resisted, so the contact angle must >90°. It is likely that there are nucleating agents dispersed throughout the body, but the pore wall cannot be a uniformly effective nucleating agent, or the freezing would go to completion at the temperature at which nucleation occurred. This point is developed in more detail elsewhere [9].

### *2.8. Growth of a flaw*

The preceding analysis shows that substantial stresses can be generated by a crystal growing in a pore. However,

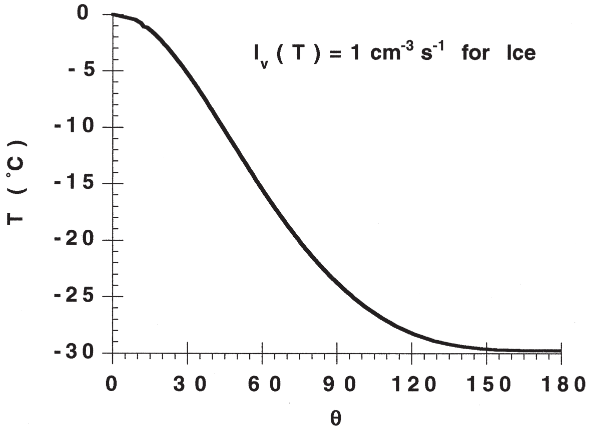

Fig. 7. Temperature at which heterogeneous nucleation creates one crystal of ice per cm$^3$ per s, as a function of the contact angle (θ) between ice and substrate.

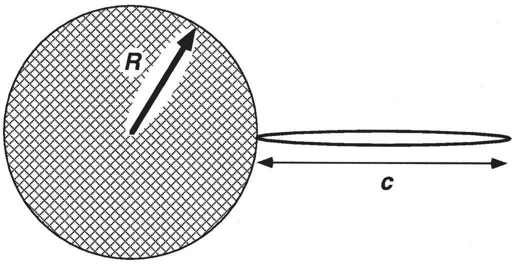

Fig. 8. Stress generated in region of radius $R$ acts on flaw of length $c$; very high stresses are required to propagate the flaw, unless $R$ is comparable in magnitude to $c$.

high stress in a single pore is not likely to cause cracking and failure of a body because the volume affected by the stress is too small. The strength of stone and concrete is controlled by the presence of very large flaws (i.e., with dimensions of tens to hundreds of microns). As a crude estimate, consider that the critical stress intensity for concrete is on the order of $K_{Ic} \approx 1$ MPa • m$^{1/2}$ [31], and it is related to the applied stress at failure, $\sigma_A$, and the flaw size, $c$ by [32]

$$K_{Ic} \approx \sigma_A \sqrt{\pi c} \tag{49}$$

Given that the tensile strength of concrete is about 3 MPa, this equation indicates a flaw size of ~3.5 centimeters! Of course, concrete is only a quasi-brittle material, so Eq. (49) does not strictly apply; nevertheless, the flaws that contribute to the low strength of concrete are very large compared to the average pore size.

For the stress generated by crystallization to act on the largest flaws, the crystals must propagate through a substantial volume of the pore space. This sort of problem has been analyzed in the context of thermal expansion mismatch in composites, where it was shown [33] that the stress field from an inclusion must extend over a distance comparable to the flaw size, or the flaw is not likely to grow. Fig. 8 shows a flaw of length $c$ adjacent to a region of radius $R$ in which stress is generated (for example, by the growth of crystals in the pores). For the two-dimensional case analyzed elsewhere [33], the tensile stress required to extend the flaw is

$$\sigma_\theta = \sqrt{\frac{8}{\pi}}\left(1 + \frac{c}{R}\right)^{3/2}\frac{K_{Ic}}{\sqrt{c}} \tag{50}$$

As indicated in Fig. 9, the stress needed to propagate the flaw drops rapidly until $R/c \geqslant 1/2$. For the crystallization pressure to act on the largest flaws in concrete, therefore, the crystals must propagate through a region many microns in length, which is enormously larger than the pore size.

If a crystal nucleates in a large pore, or penetrates from the exterior of the body into the largest pore, it will advance a relatively short distance before encountering a constriction that it cannot pass. That is, the largest pore does not percolate through the body, so the driving force (supersaturation or undercooling) that permits the crystal to enter that pore does not allow crystals to advance very far. The crystal will be arrested at the constriction until the driving force increases to the point that it can pass on to the next smaller constriction. For the crystal to advance arbitrarily deeply into the body, the driving force must be sufficient for the crystal to pass through the breakthrough radius, $r_{BT}$. This is the radius of the largest opening leading into a percolating network of larger pores; it is the characteristic pore size that controls the permeability [34] and it corresponds roughly to the inflection point in a mercury-intrusion [35] or nitrogen-desorption [36] curve. Thus, the crystallized region cannot become large enough to interact with the largest flaws until the driving force permits the crystal to pass pore entries with radii $\leqslant r_{BT}$. During freezing, Eq. (27) indicates that this would require an undercooling, given by Eq. (51):

$$\Delta T \approx -\frac{2\gamma_{cl}\cos(\theta)}{r_{BT}\Delta S_{fv}} \tag{51}$$

whereas for crystallization of salt, Eq. (19) requires a supersaturation given by Eq. (52).

$$\frac{C}{C_0} \approx \exp\left[-\frac{2\gamma_{cl}\cos(\theta)}{r_{BT}}\left(\frac{v_c}{R_g T}\right)\right] \tag{52}$$

The resulting tensile stress is given by Eq. (44) with $r_p = r_{BT}$.

## 3. Discussion

While the driving forces for crystal growth have long been understood, the mechanism by which a crystal generates stress in a pore has caused occasional confusion (e.g., [37]). We have shown that when the contact angle exceeds 90°, there is hoop tension in the pore walls; the stress arises from the fact that the pore walls must apply a stress to the crystal to suppress its growth in the radial direction. If $\theta < 180°$, then there is direct contact between the crystal and the wall and the crystal exerts a static pressure; if a crack occurs in the wall, and there is no source of liquid to allow contin-

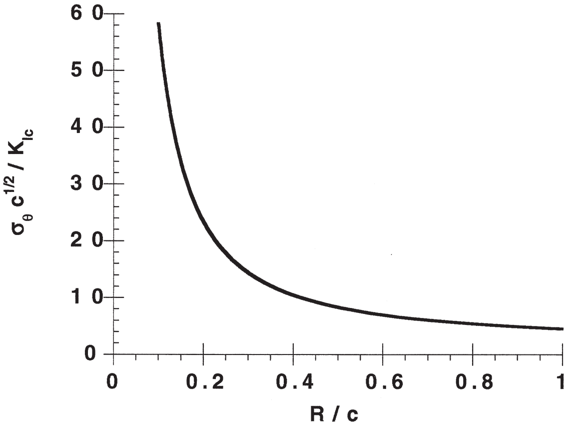

Fig. 9. Normalized hoop stress required to cause growth of flaw, as function of relative size of flaw *(c)* and region of stress *(R)*, calculated from Eq. (50).

ued growth of the crystal, then the crystallization pressure can be relieved. When $\theta = 180°$, a liquid film can be sustained between the crystal and the wall, which allows renewed growth of crystal even if cracks do appear; therefore, the crystal can sustain a load on the body even as it cracks and yields. This phenomenon is probably responsible for the increasing expansion at constant temperature observed by Powers and Helmuth [38]. The existence of an unfrozen liquid film ~1-nm thick between ice crystals and solid surfaces is clearly established by experiments including particle pushing [17], calorimetry [13], neutron diffraction [39], and nuclear magnetic resonance [40]. The best evidence for a liquid film between salt crystals and solids comes from direct measurement of pressure exerted by crystals against obstacles [26,41–43].

The upper bound on the pressure generated by a crystal is set by the driving force (undercooling or supersaturation), but the actual pressure exerted depends on many factors. Most important, if the contact angle between the crystal and the pore wall is low, then the stress can be small; if $\theta < 90°$, crystallization could even create compressive stress in the body. This suggests a method for protecting structures against crystallization damage [43]: apply a coating to the pores that reduces θ. The crystallization pressure is also small if the pore size is large, as indicated by Eq. (44); that is why frost heave is more severe in fine soils, which have small pores [15]. The pore walls only need to exert enough stress so that the pressure inside the crystal is uniform, and the total pressure is dictated by the pore size, according to Eq. (25).

The results of Section 2.6 indicate that shear or buckling of acicular crystals is unlikely, but the stress they generate is limited by their small area of contact with the wall. It has been argued [44] that acicular crystals of ettringite could generate stress efficiently by nucleating at the tips of preexisting cracks, and thereby exerted stress at a point of weakness. However, if a crystal is capable of exerting stress, then it must have a high contact angle with the wall, and in that case nucleation at a crack tip is highly improbable since that would maximize contact of the crystal with the repulsive surface. In the case of ettringite, it seems likely that compact crystals occurring in small pores generate more swelling pressure than the long needles seen in open cracks. It is also important to recognize that if a single needle of ettringite were oriented parallel to the crack surface, so that it was not under stress, then it would grow at the expense of the crystals perpendicular to the crack; the unstressed crystal would consume the supersaturation and prevent the other crystals from pushing the crack open.

There are other phenomena that can cause swelling and cracking of concrete, such as the alkali-silica reaction [45]. In general, if there is a chemical potential driving an expansive reaction, then it can be suppressed by an applied pressure, and when the reaction occurs within a pore, the pore walls will provide a portion of that pressure. Calculating the resulting stresses requires understanding of the thermodynamics of the process, as well as knowledge of the viscoelastic properties of the product and a realistic model of the pore geometry.

## 4. Conclusions

1. An upper bound on the crystallization pressure is set by the supersaturation or undercooling.
2. The actual stress can be lower than indicated by the upper bound, if the contact angle between the crystal and pore wall is low; if $\theta < 90°$, no tensile stresses result. This suggests that surface coatings might be an effective method for avoiding damage from crystallization [43].
3. The ability of crystals to push particles away indicates that in many systems a film of liquid is sustained between crystals and obstacles, such as pore walls. This means that contact angles of $\theta = \pi$ are common, so that a crystal can sustain a static load on the pore wall, even if the pore expands as a result of cracking.
4. The crystallization stress is lower in larger pores.
5. Fracture is not caused by crystallization in a single pore. It requires growth of the crystal through a region of the body comparable in size to the strength-controlling flaws. Therefore the driving force for growth must be sufficient to permit the crystals to pass through pores as small as the breakthrough radius, $r_{BT}$.

## Appendix: Gibbs analysis of crystallization under pressure

Gibbs ([7, p. 186] provides an expression in his Eq. (355) for the energy of a crystal under stress that can be written as

$$dU = TdS + Vd\Sigma \tag{53}$$

where Eq. (54) can be shown as [see Eq. (56)]:

$$d\Sigma = \sigma_x d\varepsilon_x + \sigma_y d\varepsilon_y + \sigma_z d\varepsilon_z + \tau_{xy} d\gamma_{xy} + \tau_{xz} d\gamma_{xz} + \tau_{yz} d\gamma_{yz} \quad (54)$$

and $\tau_{jk}$ and $\gamma_{jk}$ are shear stresses and strains, respectively; the quantity $Vd\Sigma$ represents the elastic strain energy. Gibbs' Eq. (401) [7, p. 198] expresses the same quantity in terms of the chemical potential per gram, $\mu$,

$$dU = TdS + SdT - pdV - Vdp + md\mu \quad (55)$$

where $m$ is the mass of the crystal. From Eqs. (53) and (55), the chemical potential is

$$md\mu = -SdT + pdV + Vdp + Vd\Sigma \quad (56)$$

If a crystal is exposed to a solution at pressure $p_l$ on the $z$ surface, then $\sigma_z = -p_l$; let the stress on the $x$ face be written as $\sigma_x - p_l$, so that $\sigma_x$ is the stress in excess of the liquid pressure, and similarly let the stress on the $y$ surface be $\sigma_y - p_l$. Then, recognizing that the volumetric change is [see Eq. (57)]

$$dV = (d\varepsilon_x + d\varepsilon_y + d\varepsilon_z)V \quad (57)$$

Eq. (56) becomes

$$md\mu = -SdT + Vdp_1 + V(\sigma_x d\varepsilon_x + \sigma_y d\varepsilon_y) \quad (58)$$

Thus, in terms of molar quantities, the chemical potential of the crystal is shown in Eq. [59].

$$d\mu_c = -S_c dT + v_c dp_1 + v_c(\sigma_x d\varepsilon_x + \sigma_y d\varepsilon_y) \quad (59)$$

The molar free energy of the liquid is given by Eq. (1a), so at equilibrium ($d\mu_l = d\mu_c$) [see Eq. (60)]:

$$(S_l - S_c)dT - (v_c - v_l)dp_1 + v_c(\sigma_x d\varepsilon_x + \sigma_y d\varepsilon_y) = 0 \quad (60)$$

At constant pressure ($dp_l = 0$), this leads to Eq. (10).

## References

[1] S.Z. Lewin, The mechanism of masonry decay through crystallization, in: Conservation of Historic Stone Buildings and Monuments, National Acad. Press, Washington, DC, 1982, pp. 120–144.

[2] I.S. Evans, Salt crystallization and rock weathering, Rev Géomorphologie dynamique XIX 4 (1969–70) 153–177.

[3] J. Marchand, R. Pleau, R. Gagné, Deterioration of concrete due to freezing and thawing, in: J. Skalny, S. Mindess (Eds.), Materials Science of Concrete IV, Am. Ceram. Soc., Westerville, OH, 1995, pp. 283–354.

[4] T.C. Powers, The air requirement of frost-resistant concrete, Proc Highway Res Board 29 (1949) 184–211.

[5] G. Amoroso, V. Fassina, Stone Decay and Conservation, Elsevier, New York, 1983.

[6] J. Thomson, Theoretical considerations on the effect of pressure in lowering the freezing point of water, Trans Roy Soc Edinburgh 16 (5) (1848–1849) 575–580.

[7] J.W. Gibbs, The Scientific Papers, Vol. I, Dover, New York, 1961.

[8] D.H. Everett, The thermodynamics of frost damage to porous solids, Trans Faraday Soc 57 (1961) 1541–1551.

[9] G.W. Scherer, Freezing gels, J Non-Cryst Solids 155 (1993) 1–25.

[10] F.T. Wall, Chemical Thermodynamics, Freeman, San Francisco, 1965, pp. 157–158.

[11] R. Defay, I. Prigogine, Surface Tension and Adsorption, Wiley, New York, 1966.

[12] A.W. Adamson, Physical Chemistry of Surfaces, 5th ed., Wiley, New York, 1990.

[13] M. Brun, A. Lallemand, J.F. Quinson, C. Eyraud, A new method for the simultaneous determination of the size and the shape of pores: The thermoporometry, Thermochimica Acta 21 (1977) 59–88.

[14] P.V. Hobbs, Ice Physics, Clarendon, Oxford, 1974.

[15] K.A. Jackson, B. Chalmers, Freezing of liquids in porous media with special reference to frost heave in soils, J Appl Phys 29 (8) (1958) 1178–1181.

[16] J. Lavalle, Recherches sur la formation lente des cristaux à la température ordinaire (Research on the slow growth of crystals at ambient temperature), Compt Rend 34 (1853) 493–495.

[17] A.E. Corte, Vertical migration of particles in front of a moving freezing plane, J Geophys Res 67 (3) (1962) 1085–1090.

[18] D.R. Uhlmann, B. Chalmers, K.A. Jackson, Interaction between particles and a solid-liquid interface, J Appl Phys 35 (10) (1964) 2986–2993.

[19] J. Israelachvili, Intermolecular & Surface Forces, 2d ed., Academic, London, 1992.

[20] A.W. Neumann, S.N. Omenyi, C.J. van Oss, Attraction and repulsion of solid particles by solidification fronts. 3. van der Waals interactions, J Phys Chem 86 (1982) 1267–1270.

[21] S.N. Omenyi, A.W. Neumann, C.J. van Oss, Attraction and repulsion of solid particles by solidification fronts. I. Thermodynamic effects, J Appl Phys 52 (2) (1981) 789–795.

[22] A.A. Chernov, V.L. Bronshtein, Conditions governing the repulsion of a solid particle by the solidification front of a weak electrolyte solution, Sov Phys Dokl 21 (12) (1976) 730–731 (Engl. transl.).

[23] S.P. Timoshenko, J.N. Goodier, Theory of Elasticity, 3d ed., McGraw-Hill, New York, 1970, p. 70.

[24] E.P. Popov, Introduction to Mechanics of Solids, Prentice-Hall, Englewood Cliffs, NJ, 1968, p. 533.

[25] M.F. Ashby, D.R.H. Jones, Engineering Materials 1, 2d ed., Butterworth-Heinemann, Oxford, 1996.

[26] S. Taber, The growth of crystals under external pressure, Am J Sci 41 (1916) 532–556.

[27] D.H. Rasmussen, A.P. MacKenzie, Effect of solute on ice-solution interfacial free energy; calculation from measured homogeneous nucleation temperatures, in: H.H.G. Jellinek (Ed.), Water Structure at the Water-Polymer Interface, Plenum, New York, 1972, pp. 126–145.

[28] G.G. Litvan, Phase transitions of adsorbates: III. Heat effects and dimensional changes in nonequilibrium temperature cycles, J Colloid Interface Sci 38 (1) (1972) 75–83.

[29] C. le Sage de Fontenay, E.J. Sellevold, Ice formation in hardened cement paste—I. Mature water-saturated pastes, in: P.J. Sereda and G.G. Litvan (Eds.), Durability of Building Materials and Components, ASTM STP 691, ASTM, 1980, pp. 425–438.

[30] J.W. Christian, The Theory of Transformations in Metals and Alloys, Part I, Pergamon, New York, 1975, p. 451.

[31] S. Mindess, J.F. Young, Concrete, Prentice-Hall, Englewood Cliffs, NJ, 1981, p. 361.

[32] S.P. Shah, S.E. Swartz, C. Ouyang, Fracture Mechanics of Concrete, Wiley, New York, 1995.

[33] T.C. Lu, J. Yang, Z. Suo, A.G. Evans, R. Hecht, R. Mehrabian, Matrix cracking intermetallic composites caused by thermal expansion mismatch, Acta Metall Mater 39 (8) (1991) 1883–1890.

[34] A.J. Katz, A.H. Thompson, Quantitative prediction of permeability in porous rock, Phys Rev B 34 (11) (1986) 8179–8181.

[35] A.J. Katz, A.H. Thompson, Prediction of rock electrical conductivity from mercury injection measurements, J Geophys Res 92 (B1) (1987) 599–607.

[36] H. Liu, L. Zhang, N.A. Seaton, Analysis of sorption hysteresis in mesoporous solids using a pore network model, J Colloid Interface Sci 156 (1993) 285–293; erratum 162 (1994) 265.

[37] S.Z. Lewin, The mechanism of masonry decay through crystallization, in: Conservation of Historic Stone Buildings and Monuments, National Acad. Press, Washington, DC, 1982, pp. 120–144.

[38] T.C. Powers, R.A. Helmuth, Theory of volume changes in hardened portland-cement paste during freezing, Proc Highway Res Board 32 (1953) 285–297.

[39] J.D.F. Ramsay, G. Wing, Small angle neutron scattering investigations of water sorption in porous silica and ceria gels, J Colloid Interface Sci 141 (2) (1991) 475–485.

[40] P.G. Hall, R.T. Williams, R.C.T. Slade, Nuclear magnetic resonance and dielectric relaxation investigations of water sorbed by Spherisorb silica, J Chem Soc, Faraday Trans 1 (81) (1985) 847–855.

[41] G.F. Becker, A.L. Day, Note on the linear force of growing crystals, J Geology XXIV (4) (1916) 313–333.

[42] I.S. Evans, Salt crystallization and rock weathering, Rev Géomorphologie dynamique XIX (4) (1969–70) 153–177.

[43] L. Gustafson, W. Vichit-Vadakan, G.W. Scherer, Protecting against damage from salt crystallization by control of interfacial energy, to be published.

[44] Y. Fu, P. Xie, P. Gu, J.J. Beaudoin, Significance of pre-existing cracks on nucleation of secondary ettringite in steam cured cement paste, Cem Concr Res 24 (6) (1994) 1015–1024.

[45] R. Helmuth, D. Stark, Alkali-silica reactivity mechanisms in: Materials Science of Concrete III, J. Skalny (Ed.), Am. Ceram. Soc., Westerville, OH, 1992, pp. 131–208.